APPLIED AND ENVIRONMENTAL MICROBIOLOGY, July 2005, p. 3682–3691 Vol. 71, No. 7
0099-2240/05/$08.00+0 doi:10.1128/AEM.71.7.3682–3691.2005

Survey of Motile Microaerophilic Bacterial Morphotypes in the Oxygen Gradient above a Marine Sulfidic Sediment

Roland Thar* and Tom Fenchel

Marine Biological Laboratory, University of Copenhagen, Strandpromenaden 5, 3000 Helsingør, Denmark

Received 4 August 2004/Accepted 31 January 2005

Enrichment cultures for free-swimming microaerophilic bacteria were prepared from marine sulfidic sediment samples (Nivå Bay, Denmark). We observed nine different morphotypes; three of these morphotypes represented already-described species, i.e., *Thiovulum majus*, "*Candidatus* Ovobacter propellens," and an as-yet-unnamed large vibrioid bacterium. In addition, we observed several morphotypes of spirilla and one vibrioid morphotype. A common feature of all investigated bacteria was that they aggregated chemotactically at the oxic-anoxic interface, whereas preferred oxygen concentration were in the range of 1 to 10 μM. The motile behavior and flagellar dynamics are analyzed in detail with an emphasis on spirilla.

Sulfidic marine sediments covered by air-saturated seawater are generally characterized by steep opposing oxygen and sulfide gradients within the upper millimeters of the sediment. Dissolved sulfide is produced by sulfate-reducing bacteria within the anoxic deeper sediment layers, from where it constantly diffuses upward toward the sediment surface (23). The layer several 100 μm in thickness where molecular oxygen and sulfide coexist at the oxic-anoxic interface harbors a variety of colorless sulfur bacteria, which are able to utilize the free energy obtained from the oxidation of reduced sulfur compounds (18, 25). The position of the oxic-anoxic interface often changes, e.g., due to convective water currents at the sediment surface or due to diel activity cycles of oxygenic photosynthesis (24). Thus, many colorless sulfur bacteria are highly motile in order to follow their preferred position within the oxygen gradient.

If the oxic-anoxic interface is positioned within or directly at the surface of the sediment, species of colorless sulfur bacteria relying on surface associated motility are often abundant in high numbers (e.g., *Beggiatoa* spp. showing gliding motility or *Achromatium* spp. showing "rolling" motility) (21, 31). However, if the sulfide production within the sediment is sufficiently high, the oxic-anoxic border moves above the sediment surface. Provided that the overlaying water is constantly mixed and air saturated, this border will be positioned within the diffusive boundary layer covering the sediment surface. The thickness of this layer measures typically several 100 μm (26). In this case only microaerophilic bacteria relying on free-swimming motility can keep their position at the oxic-anoxic interface.

Long known and best described among these free-swimming species in marine environments is *Thiovulum majus* (19, 27, 42), whereas in recent years we described two additional new species: "*Candidatus* Ovobacter propellens" (20) and a large vibrio (designated NivaVib1 here) (39, 40). None of these species have thus far been isolated in pure culture, most probably because the complex gradient system of their natural environment could not be mimicked sufficiently by the applied culturing techniques (40, 42). During our previous studies we became aware that enrichment cultures for these three species often also harbored several other species of free-swimming microaerophilic bacteria, mostly spirilla. The present study gives an overview of the additional species, with emphasis on their morphology and motility behavior.

* Corresponding author. Mailing address: Marine Biological Laboratory, University of Copenhagen, Strandpromenaden 5, 3000 Helsingør, Denmark. Phone: 45-49-21-33-44. Fax: 45-49-26-11-65. E-mail: rthar@bi.ku.dk.

MATERIALS AND METHODS

Enrichment culture. Sulfidic sediment mixed with decaying seagrass and macroalgae was sampled from a marine sulfuretum with brackish water located in Nivå Bay (25 km north of Copenhagen) and transported within 1 h to the laboratory. The sediment was filled into open petri dishes (250 mm in diameter, 150 mm in height, no cover lid) and placed into an aquarium filled with seawater (15 to 20 ppt salinity) from the sampling site (see Fig. 8A). The setup was kept at room temperature and exposed to dim daylight. The water was constantly aerated causing advective currents with flow velocities of ca. 5 mm s^{-1} above the sediment surface, which ensured the long-term stability of the sulfide and oxygen gradients at the sediment surface. Enrichment cultures could be kept for several months by burying three sheets of Kleenex tissues in the sediment every 2 to 3 weeks, which provided organic nutrients for the heterotrophic bacterial population in the anoxic sediment layers.

Flagellation. The flagellation of species with thick flagellar bundles could be directly observed by light microscopy using phase contrast or differential interference contrast (DIC). Otherwise, bacteria were transferred onto a transmission electron microscopy (TEM) grid covered with support film and fixed with OsO_4 vapors. After drying, the prepared grid was inspected by a transmission electron microscopy (full-mount TEM; Zeiss EM 900).

Flat-glass capillary preparations. The motility behavior within steep oxygen gradients was investigated in flat-glass capillary preparations. Sediment surface samples containing gradient bacteria were taken from the enrichment culture with the help of a Pasteur pipette and filled into the center of flat glass capillaries (8 by 0.8 by 40 mm inner dimensions; VitroCom, Inc., Mountain Lakes, N.J.). The remaining space in the capillaries was filled with seawater from the enrichment culture. The respiration of the bacteria ensured that the inner part of the capillary became anoxic within 20 to 40 min. The investigated gradient bacteria accumulated within the steep oxygen gradients at either end of the capillary, where their motility behavior was investigated by combined video microscopy and microsensor measurements. Alternatively, one side of the capillary was filled with a sulfidic agar plug prepared from filtered seawater, 1% agarose, and neutralized sodium sulfide solution (final concentration, 1 mM H_2S). The sulfidic agar plug maintained a stable sulfide-oxygen counter-gradient within the capillary for 24 h.

Oxygen gradient measurements. Dissolved oxygen gradients were measured with Clark-type oxygen microsensors with a guard cathode (35) connected to a Picoammeter (Unisense A/S, Århus, Denmark). The microsensors had a tip diameter of 10 to 20 μm and a <2% stirring sensitivity. A linear two-point

calibration was performed in air-saturated and in anoxic seawater from the enrichment culture. The microsensor was horizontally mounted on a micromanipulator (Märzhäuser Wetzlar, Wetzlar-Steindorf, Germany), and its tip was inserted into the flat glass capillary containing the bacterial samples. The position of the microsensor tip relative to the bacterial bands was documented by video microscopy.

Video microscopy and motion analysis. Either a standard black-and-white charge-coupled device (CCD) video camera (25-Hz frame rate, EHD kam pro; EHD GmbH, Damme, Germany) or a high-speed CCD camera (up to 1,000-Hz frame rate, CPL-MS1000 CCD; Canadian Photonic Lab, Minnedosa, Canada) was connected to the video-tube of a microscope using either phase contrast or DIC. Motion analysis was done by replaying the recorded movies on a screen (~30 cm in diameter) overlaid with transparent sheets. Cell position and flagellar configurations of consecutive frames were redrawn manually on the transparent sheets. The obtained cell tracks were analyzed for swimming velocity, turning angles, cell distribution in oxygen gradients, rotation rates of cells and flagella, and flagellar beating patterns. Only cells with tracks lying within the focal plane were taken into account.

Spatial heterogeneity of species composition. A metal grid (120 by 80 mm, 10-by-10-mm cell size) was placed 1 cm above the sediment surface of an enrichment culture. The tip of a 1-ml Eppendorf pipette was carefully positioned on the sediment surface at the center of a grid cell. A volume of 0.1 ml was sucked into the pipette and transferred onto a microscope slide. The order of magnitude of cell numbers in this preparation was determined by light microscopy (10× phase). This procedure was repeated for each grid position.

RESULTS

Morphotypes. During the period between January and June of 2004, sulfidic sediment samples from Nivå bay were collected about every 4 weeks for enrichment cultures in the laboratory. The sediment surface of the enrichment cultures were weekly screened by flat-glass capillary preparations for the species composition of free-swimming microaerophilic bacteria. Altogether, we observed nine different morphotypes (Fig. 1 and Table 1), each of them was found repetitively during the period of observation. Three of them represented conspicuous bacterial species, which have been described in former publications, i.e., NivaVib1 (39, 40), "Ovobacter propellens" (20), and *Thiovulum majus* (10, 17, 42). Therefore, the present study concentrates on the remaining six new morphotypes comprising five spirilla (NivaSpi1-NivaSpi5) and one vibrio (NivaVib2).

The four bigger spirilla NivaSpi1-NivaSpi4 could be unequivocally distinguished by the geometry of their spirilloid cell shape (Table 1). In addition, NivaSpi2 and NivaSpi3 showed bipolar flagellar bundles (monopolar directly after cell division) that were clearly visible by phase-contrast or DIC microscopy (Fig. 1). The most prominent feature of NivaSpi4 were brownish, strongly light scattering iron depositions on the cell surface (Fig. 1). The remaining morphotypes, which were less than 3 μm in size, were classified by their spirilloid (NivaSpi5) or vibrioid (NivaVib2) shape. All morphotypes proliferated by binary cell division.

Motility behavior in oxygen gradients. The bacteria formed dense, 100- to 200-μm-thick bands at the oxic-anoxic border (e.g., Fig. 2A and B); the bands were often easily recognizable by eye. Occasionally, the bands were dominated by a single morphotype, but in most cases they consisted of a mixture of morphotypes. The dissolved oxygen concentration at the center of the bands within the oxygen gradient varied between 1 and 10 μM. However, within a single flat-glass capillary preparation NivaSpi1-NivaSpi5, NivaVib1, NivaVib2, and "*Ca*. Ovobacter" gathered at the same position within the oxygen gradient. The only exception was *Thiovulum*, which was found at higher oxygen concentrations of ca. 10 μM. Within oxygen gradients steeper than ca. 100 μM mm^{-1}, cells of all nine morphotypes were able to accumulate in the bands. Within weak oxygen gradients of less than ca. 10 μM mm^{-1}, motile cells of NivaVib1 were scattered randomly along the whole length of the flat-glass capillary, whereas cells of NivaSpi1-NivaSpi5 and NivaVib2 formed the usual sharp band at the oxic-anoxic border (e.g., Fig. 2C).

Cells within the bands were constantly moving. The motility pattern of NivaSpi1-NivaSpi5 could be described as a "run and reverse" pattern: cells approaching either border of the band stopped and started moving again in the opposite direction, i.e., the anterior cell end became the posterior cell end and vice versa. Thus, the effective turning angle of the cell tracks peaked around 180°, with typically >50% of the turning angles lying between 170° and 190° (Fig. 3). In contrast, the vibrioid cells of NivaVib2 showed random directional changes (Fig. 3).

Generally, inward swimming speeds, i.e., speed of cells swimming toward the anoxic region, did not differ from outward swimming speeds. However, cells from NivaSpi1 showed significantly (>200%) increased inward swimming speeds compared to the outward ones (Table 1). This characteristic behavior allowed easy recognition of NivaSpi1 when observed under the light microscope. The relationship between swimming speeds, v, and rotation rates, r, of the cells along their long axis were investigated for NivaSpi1-NivaSpi3. For these morphotypes there was a direct linear dependence, i.e., $v = kr$, where k is a morphotype-specific constant in micrometer units (Fig. 4).

The flagellar bundles of two morphotypes, NivaSpi2 and NivaSpi3, were visible in phase-contrast light microscopy. Thus, it was possible to study the dynamics of the spirilla and their flagella in detail by high-speed video microscopy. During straight runs, the helical cell body (comprising a right-handed helix as could be concluded by moving the focal plane up and down) rotated counterclockwise if viewed from the anterior end. The posterior flagellar bundle was aligned with the cell body, whereas the anterior bundle was bent backward along the cell body (Fig. 5).

The rotation of both flagellar bundles always started and ceased simultaneously. When it ceased, it always was followed by a reversal of swimming direction. The actual reversal takes place within ca. 100 ms (Fig. 6). After both bundles stopped rotating, the cell lies motionless for 83 ± 57 ms (mean ± the standard deviation for NivaSpi3 [$n = 8$]) only affected by Brownian motion. After this resting period, the cell starts again rotating in the opposite direction. Within ca. 30 ms the formerly anterior bundle unfolds and gets aligned with the cell body, becoming the anterior bundle for the new swimming direction (Fig. 6). Simultaneously, the formerly posterior bundle bends backward along the cell body becoming the anterior bundle.

We investigated whether the reversal position is dependent on the effective swimming speeds, v_{eff}, along the oxygen gradient (see Discussion). The effective swimming speed is defined as the velocity component parallel to the gradient, $v_{eff} = v \cos(\alpha)$, where v represents the total swimming speed and α represents the angle between swimming direction and the direction of the gradient. The data obtained for NivaSpi3 did not

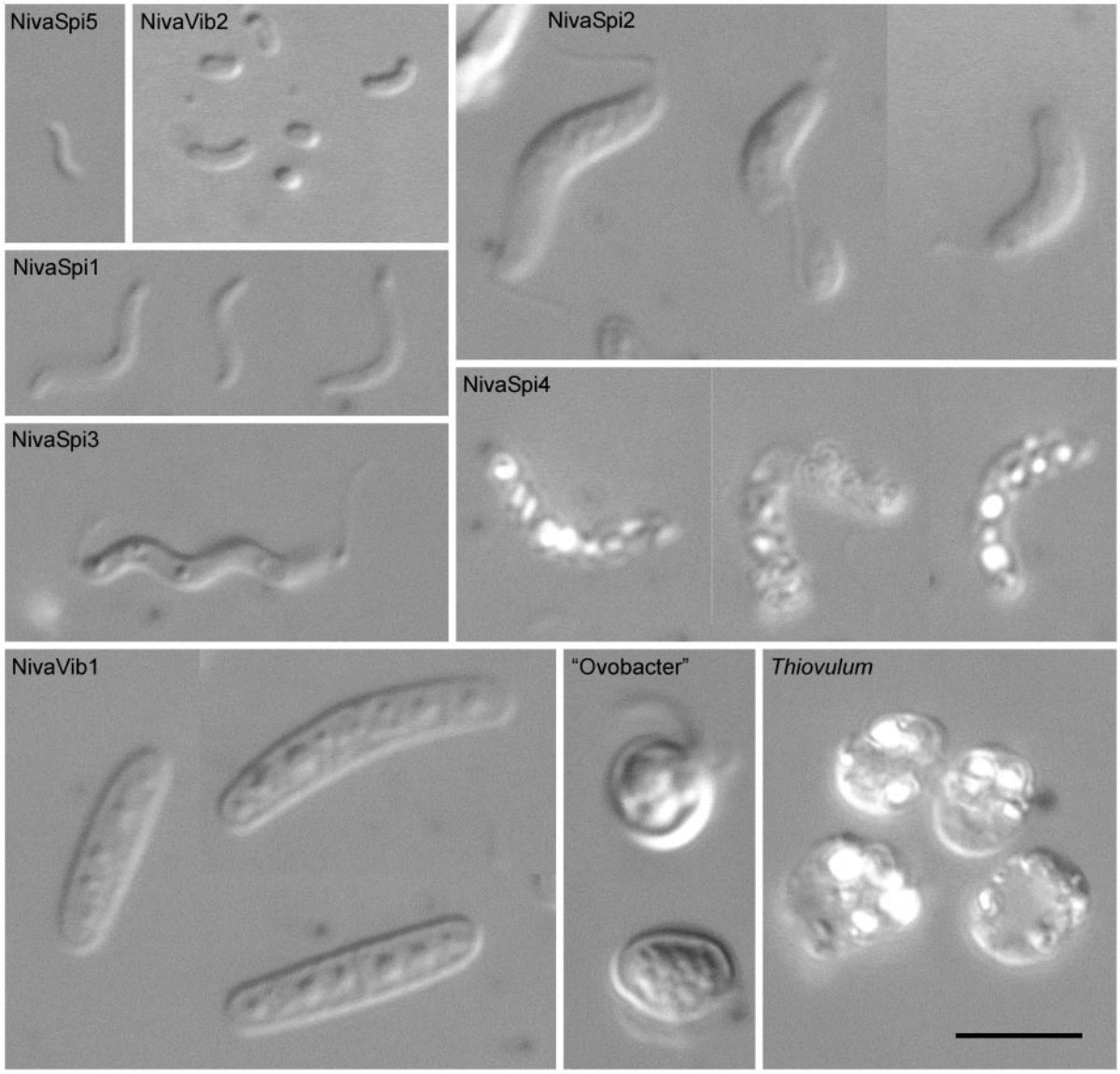

FIG. 1. Observed morphotypes of motile microaerophilic bacteria inhabiting the oxic-anoxic interface above sulfidic sediments (cells fixed with glutaraldehyde). All photographs were taken under identical magnification and illumination conditions (magnification, ×1,000 [DIC light microscopy]). Flagellar bundles are visible for NivaSpi2, NivaSpi3, and "*Ca*. Ovobacter propellens." NivaSpi3, NivaVib1, and "*Ca*. Ovobacter propellens" show spherical refractile inclusions. Brownish light-scattering iron depositions (presumably ferric hydroxide) can be seen on NivaSpi4, whereas *Thiovulum* possesses bright light-scattering sulfur inclusions. Scale bar, 5 μm.

indicate any dependence between effective swimming speed and reversal position; rather, the reversal positions lay around an oxygen concentration of 15.4 ± 4.6 μM (mean ± the standard deviation [$n = 15$]) (Fig. 7).

In addition to the "run and reverse" motility pattern, another band-forming mechanism was found for NivaSpi3. In some flat-glass capillary preparations (about 1 out of 10 preparations) they attached by a mucous stalk to debris particles. The long axis of attached spirilla was always aligned with the oxygen gradient, with the nonattached end pointing toward the oxic side. Attached cells continually rotated along their long axis. If the oxic-anoxic interface moved outward, the attached cells kept their position within the oxygen gradient by elongation of their stalks. In this way, the stalks of many spirilla built up a whitish, fibrillar, mucous fabric, which was clearly visible by light microscopy. Within 30 min such a mucous fabric could extend over several 100 μm. However, in most preparations cells of NivaSpi3 remained free-swimming and did not attach.

Temporal and spatial heterogeneity. The enrichment cultures showed temporal as well as spatial heterogeneity. Temporal heterogeneity was most pronounced for the bigger morphotypes. The spirilla showing the iron deposits were mostly found in enrichment cultures within the first days after collection of the sediment samples from the natural habitat. For *Thiovulum*, "*Ca*. Ovobacter propellens," NivaVib1, and NivaSpi1 we repeatedly observed mass occurrences, which lasted for several days. Cells belonging to the smaller morphotypes NivaSpi5 and NivaVib2 were always abundant. In contrast,

TABLE 1. Characteristics of the investigated free-swimming microaerophilic bacteria[a]

Bacterium[d]	Cell shape	Cell length (μm)	Cell diam (μm)	Wave length of spirilloid shape (μm)	Flagellation[b]	Swimming speed (μm s^{-1})	Motility behavior	Preferred O_2 concn (μM)	Inclusions or depositions	Mucous stalk
NivaSpi1	Helical	6.6 ± 0.9	~0.5	~5	Mono- or bipolar, up to 10 μm long, not visible	Out, 60 (30–100); in, 140 (80–250)[c]	Run and reversal	1–10	None	No
NivaSpi2	Helical	9.4 ± 1.0 (8–11)	1.9 ± 0.1	9.2 ± 0.6	Mono- or bipolar bundles, visible	200 (100–350)	Run and reversal	1–10	None	No
NivaSpi3	Helical	9.0 ± 2.2 (6–12)	1.1 ± 0.1	4.0 ± 0.2	Mono- or bipolar bundles, visible	180 (80–300)	Run and reversal, threshold sensing	1–10	Spherical refractile inclusions, diam ca. 0.3 μm	Yes
NivaSpi4	Helical	8.0 ± 0.7	1.7 ± 0.3	~15	Not visible	200 (100–350)	Run and reversal	1–10	Light-scattering brownish depositions, diam up to 2 μm	No
NivaSpi5	Helical	2.8 ± 0.1	0.8 ± 0.1	~3	Not visible	130 ± 20	Run and reversal	1–10	None	No
NivaVib2	Vibrioid	2.3 ± 0.1	1.3 ± 0.1		Monopolar, not visible	135 ± 25	Run and tumble	1–10	None	No
NivaVib1*	Vibrioid	~6 (4–10)	1.3–2.5		Bipolar bundles, not visible	~75	Boomerang tracks, true chemotaxis, probably spatial sensing	~2	Spherical refractile PHB inclusions, diam up to 2 μm	Yes
"Ovobacter propellens"*	Ovoid		4–5		Huge monopolar flagellar tuft, visible	650 (200–1,000)	Helical tracks, run and U-turn	~2	Numerous refractile PHB inclusions in central vacuole, diam up to 2 μm	No
*Thiovulum majus**	Spherical		5–25		Peritrichous, not visible	250 (150–600)	Helical tracks, run and U-turn or true chemotaxis by helical klinotaxis	~10	Light-scattering sulfur inclusions	Yes

[a] Values are given either as an average ± the standard deviation ($n > 10$) or as an average together with the range from the minimal to maximal values.
[b] "Visible" means observable by phase-contrast light microscopy.
[c] "Out" corresponds to swimming direction toward the oxic region; the reverse is true for "in."
[d] *, data were obtained from references 7, 14, 17, 35, 36, and 38.

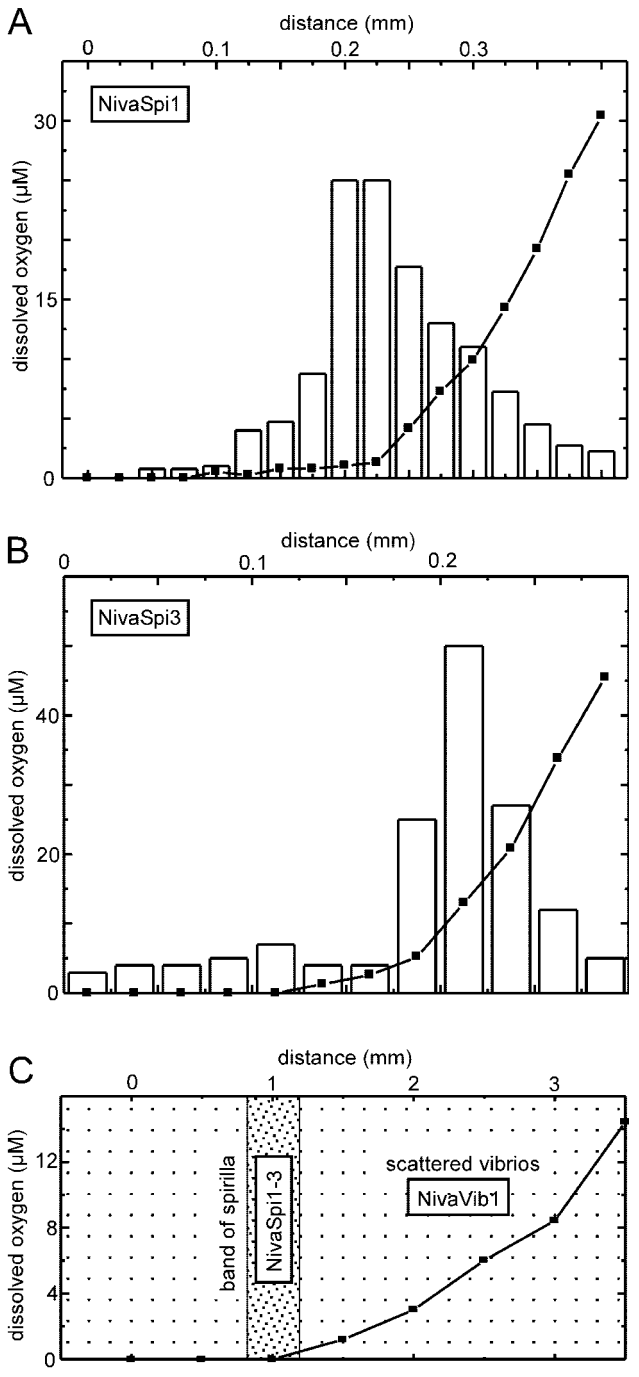

FIG. 2. Relative cell distribution (open bars) of different morphotypes in oxygen gradients (black squares). Each graph represents an individual flat-glass capillary preparation. (A and B) Narrow bands < 200 μm in thickness of NivaSpi1 (A) and NivaSpi3 (B) at the oxic-anoxic border. (C) Preparation with shallow oxygen gradient. NivaSpi1 to -3 are aggregated in a narrow band at the oxic-anoxic interface, whereas NivaVib1 is randomly scattered.

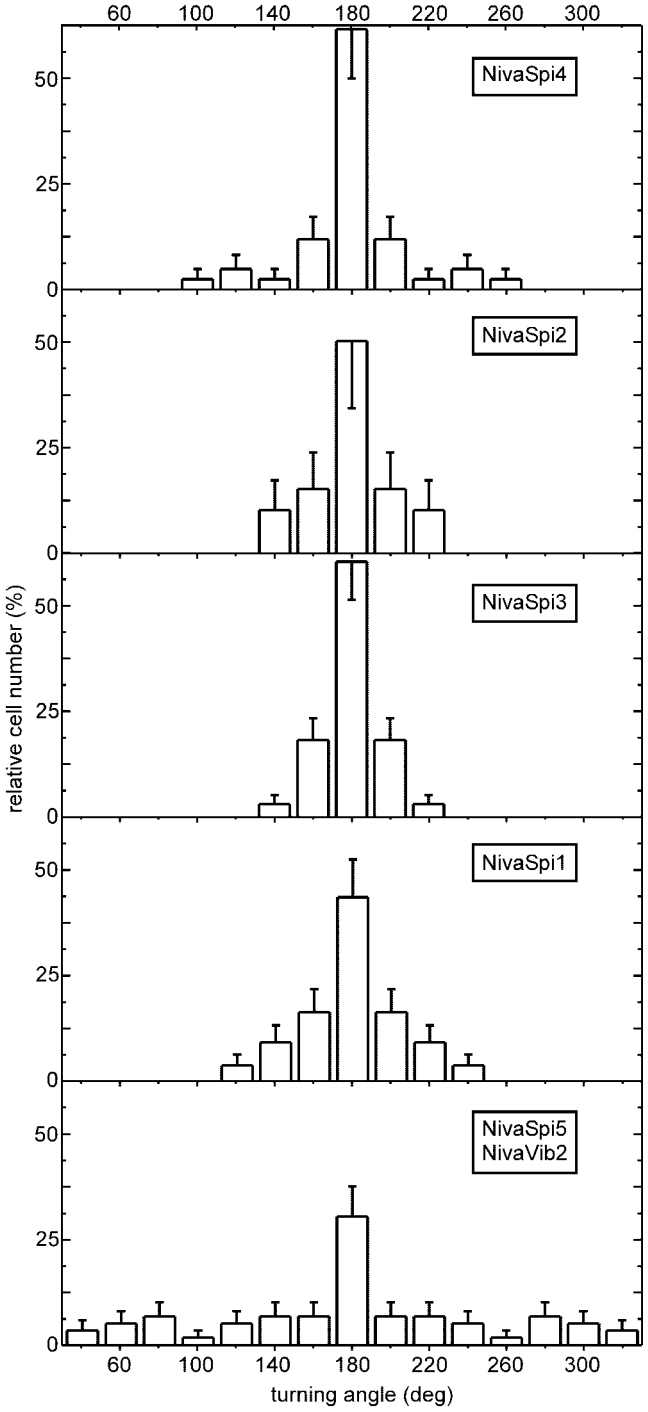

FIG. 3. Distribution of turning angles for the different morphotypes. Error bars indicate the standard deviations. Due to their small size, NivaSpi5 and NivaVib2 could not be distinguished by the tracking procedure. Therefore, their turning angles are combined in the lowest panel. However, direct visual inspection of their motility behavior showed that NivaSpi5 mostly contributed to the peak at 180°, whereas NivaVib2 showed random directional changes.

cells of NivaSpi3 and NivaSpi2 were only found occasionally and were always outnumbered by other morphotypes.

Horizontal heterogeneity was observed on the sediment surface of the enrichment culture at a scale of centimeters. Figure 8 shows the horizontal distribution of microaerophilic bacteria in an enrichment culture, at a time when *Thiovulum*, NivaSpi1, NivaSpi2, and NivaSpi4 were absent or rare. The center of the enrichment culture was dominated by NivaVib1 (as can be anticipated by the whitish mucous veils built up by NivaVib1

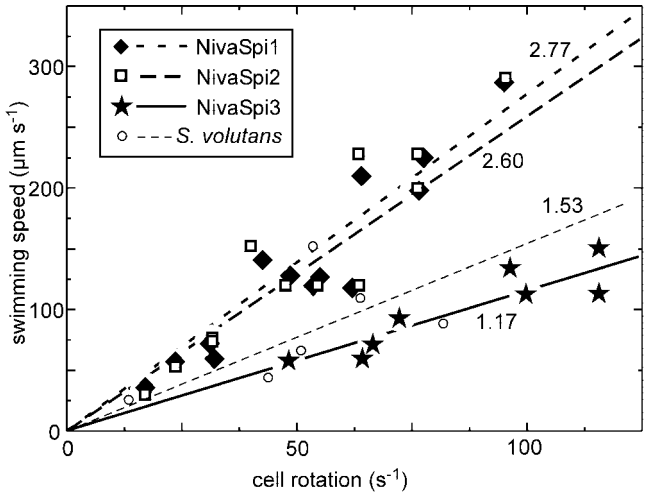

FIG. 4. Observed relationship between cell rotation rate and swimming speed for the spirilla NivaSpi1-NivaSpi3 (dots), together with linear curve fits crossing the origin (lines, $r^2 > 0.8$). The numbers next to the curve fits gives their steepness in units of micrometers. In addition, the literature data for *Spirillum volutans* are shown (30).

[Fig. 8A]) accompanied by the small morphotypes NivaSpi5 and NivaVib2 (Fig. 8B). This region was surrounded by a zone with highly abundant "*Ca*. Ovobacter" cells, whereas the outer regions were dominated by *Beggiatoa* spp. and *Achromatium* sp. (presumably *Achromatium volutans*). The spirilla of NivaSpi3 showed very low abundance (Fig. 8B).

DISCUSSION

Our screening revealed nine different morphotypes of free-swimming microaerophilic bacteria. The seven morphotypes showing cell lengths of >5 μm most probably represent monophyletic species, since they can be differentiated by many unique features of their morphology and motility behavior (Table 1). This conclusion does not hold for the two smallest morphotypes, NivaSpi5 and NivaVib2, so they might in fact represent a mixture of species. Three morphotypes could be identified as species that have been described in detail in literature, i.e., *Thiovulum majus* (10, 17, 42), "*Ca*. Ovobacter propellens" (20), and NivaVib1 (39, 40). Members of the spirilla NivaSpi1 to -5 might be related to members of the genera

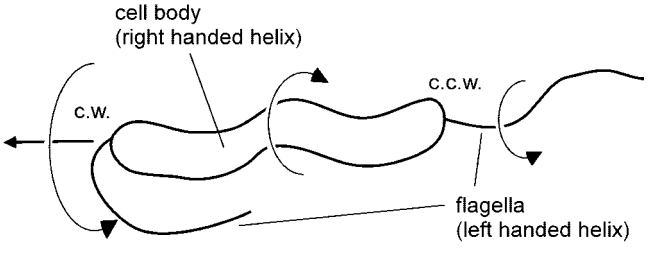

FIG. 5. Dynamics of a straight-swimming spirillum with bipolar flagella. The straight arrow indicates the swimming direction, curved arrows designate rotation directions of the cell body and the flagella. The terms c.w. (for clockwise) and c.c.w. (for counterclockwise) specify the rotation direction of the flagellar motors relative to the cell membrane (if seen from outside the spirillum).

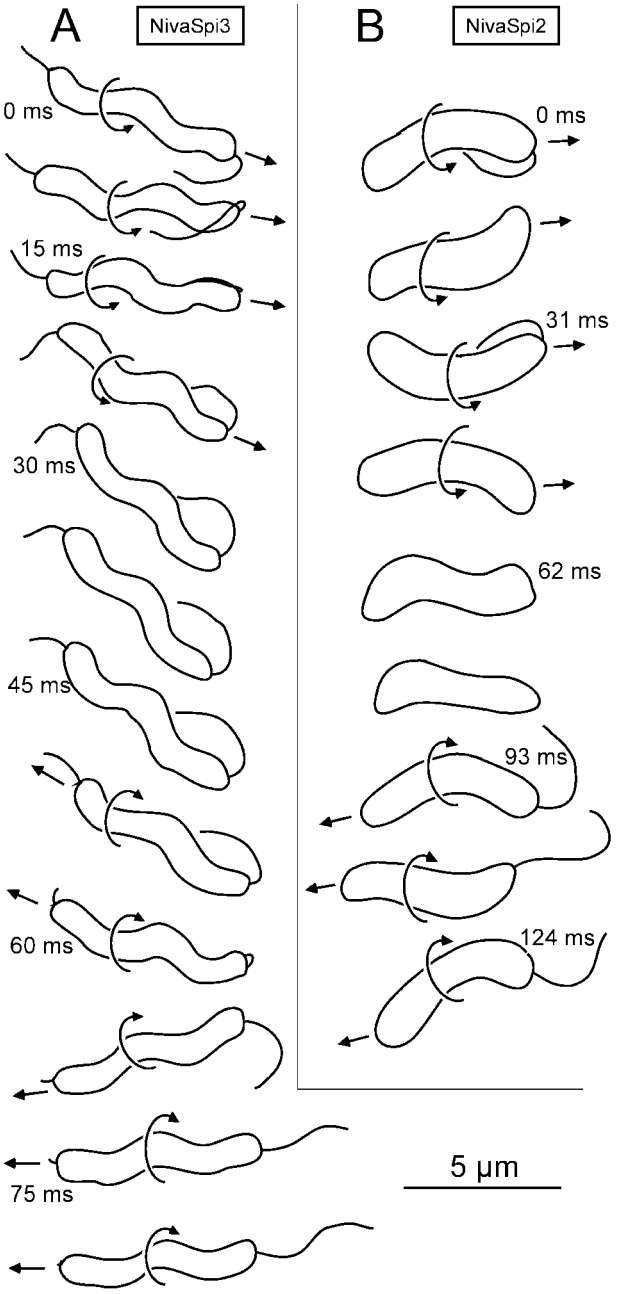

FIG. 6. Dynamics of a reversing spirillum of NivaSpi3 (A) and NivaSpi2 (B). Drawings outline the configuration of the cell body and the flagellar bundles at equidistant time points (given in milliseconds next to every second drawing). Straight and curved arrows indicate swimming direction and rotation direction of the cell body, respectively.

Spirillum or *Aquaspirillum*; for example, *Spirillum winogradskyi* and *Aquaspirillum bipunctata* (both formerly belonging to the genus *Thiospira*) have been described to aggregate chemotactically at the interface of opposing oxygen and sulfide gradients (11, 12, 29). However, the characteristic feature of both species are light-scattering sulfur inclusions, which were never observed for any spirillum in our present study. It is unlikely that this absence of sulfur inclusions was due to environmental

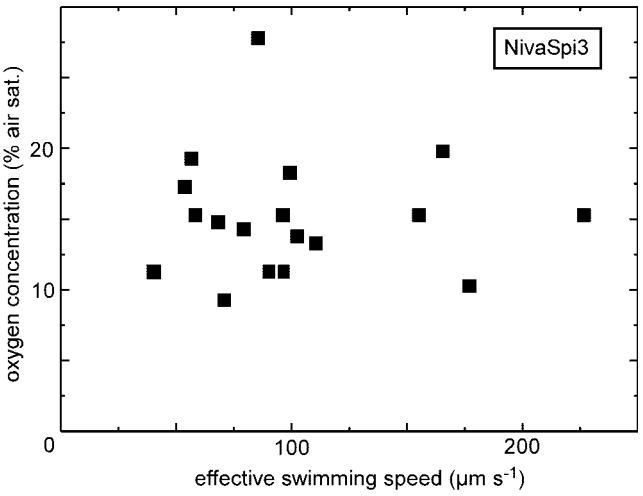

FIG. 7. Effective swimming speed (i.e., velocity component parallel to the oxygen gradient) of NivaSpi3 plotted against the oxygen concentration of the reversal positions at the oxic border of the bacterial band.

conditions (e.g., low abundance of reduced sulfur compounds in the surrounding water) because cells of *Thiovulum* always showed a high content of sulfur inclusions.

The chemotactic aggregation of the described morphotypes at the oxic-sulfidic interface points to a metabolism that is related to the oxidation of reduced sulfur compounds. However, thus far, this has only been proven for *Thiovulum* (42). It cannot be excluded that some morphotypes represent, e.g., microaerophilic organoheterotrophic species, since the eutrophic sediment in the enrichment cultures will also give rise to opposing gradients of dissolved organic compounds and oxygen.

The morphotype NivaSpi4 is an exception from these considerations. The observed brownish light-scattering depositions resemble descriptions of ferric hydroxide depositions found in iron-oxidizing bacterial mats (15, 16). In fact, two spirilloid iron-oxidizing bacteria have been isolated, which formed bacterial plates within opposing gradients of ferrous sulfide and oxygen (14). They were tightly associated with ferric hydroxides depositions. The common features suggest that NivaSpi4 is related to these isolates. NivaSpi4 was only observed in freshly sampled enrichment cultures. The fresh sediment samples probably contained sufficient ferrous iron for NivaSpi4, whereas after some days the ferrous iron pool was removed by oxidation and deposited as ferric hydroxides.

Chemotactic strategy. Bacterial chemotaxis is best understood from studies with *E. coli*. It can be briefly described as a "run and tumble" strategy: straight swimming paths are interrupted by random directional changes (random walk). When *E. coli* senses increasing concentrations of an attractant along its swimming path, the probability for a tumble event is decreased, which results on average in a migration toward the attractant (biased random walk) (5, 7). In our study, only the small vibrioid morphotype NivaVib2 showed a "run and tumble" strategy, as can be expected from the random directional changes (Fig. 3).

All other morphotypes used different chemotactic strategies. Those used by *Thiovulum* (19, 38), "*Ca*. Ovobacter" (20), and NivaVib1 (39) were described in earlier publications. The remaining morphotypes represent all spirilla showing a "run and reverse" strategy, a feature which has often been observed for motile marine bacteria (3, 4). It has been shown that a "run and reverse" strategy is advantageous for microenvironmental conditions typical for marine bacteria (2, 4, 30). This is obviously true in our case of one-dimensional oxygen gradients. The 180° directional changes ensure that the spirilla have a 100% chance of returning to their aggregation band from either side. In contrast, a random change in direction would allow the spirilla only a 50% chance to return to their aggregation band by a single directional change (Fig. 2).

Chemotaxis of *E. coli* is based on temporal sensing, i.e., the bacterium does not react to the absolute attractant concentration; rather, it senses temporal concentration changes (1, 7). If the spirilla in our study also relied on temporal sensing, then the reversal position within the oxygen gradient should be dependent on the effective swimming speed along this gradient. That is, spirilla with fast effective swimming speeds should reverse sooner when approaching the band borders than spirilla with lower effective swimming speeds. However, our investigation of this issue for the spirillum NivaSpi3 revealed no obvious relationship between effective swimming speed and reversal position in the oxygen gradient (Fig. 7). Rather, the reversal at the oxic border occurred around a threshold oxygen concentration of 15 μM. Therefore, the sensing principle of NivaSpi3 should be termed "threshold sensing." The advantage of threshold sensing might be that it requires less complex intracellular signaling mechanisms than temporal sensing. The latter requires some kind of memory for detecting temporal concentration changes, as well as some adaptive mechanism in order to cope with attractant concentration varying over several orders of magnitude (1, 7). In contrast, threshold sensing needs neither a memory nor an adaptive mechanism.

An earlier publication (39) on the chemotactic behavior of NivaVib1 demonstrated that these bacteria most likely utilize spatial gradient sensing. This mechanism would be based on two independent sensor regions at either end of the vibrioid cell. The bacterium would sense the oxygen gradient along its cell body by comparing the signals of both sensor regions. It was experimentally shown that NivaVib1 could sense a difference in oxygen concentration of 0.2 μM along their cell bodies (39). In the present study we observed that NivaVib1 is not able to aggregate in a band when the oxygen gradient is as low as 3 μM mm^{-1} (Fig. 2C). This corresponds to a maximal concentration difference of ca. 0.02 μM between the two ends of the cell. This value comes close to the theoretical noise limit calculated for spatial sensing (39); thus, NivaVib1 was no longer able to orient itself in the oxygen gradient. In contrast, the spirilla could aggregate in a band by threshold sensing (Fig. 2C).

Motility mechanisms of spirilla. The hydrodynamics of bacteria are characterized by low Reynolds numbers (33), for which inertial forces can be neglected. In this regime, the motion of a spirillum through water can be envisaged by a screw penetrating a piece of wood (9, 34). The necessary torque is produced by the flagellar motors at either end of the spirillum (6). The standard conformation of bacterial flagella resembles a left-handed helix (41). Since the cell body and the

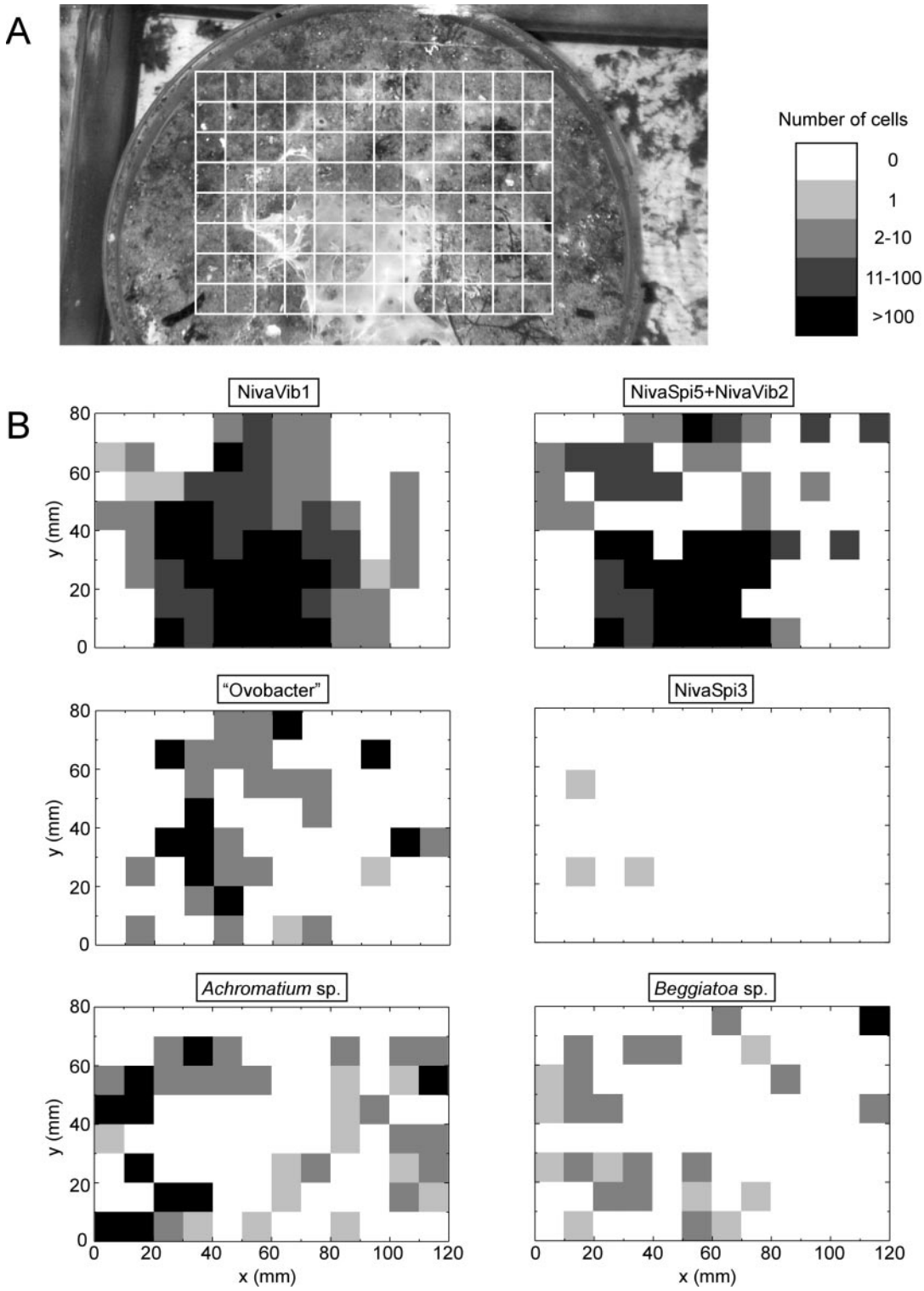

FIG. 8. Spatial heterogeneity of an enrichment culture. (A) Top view of enrichment culture overlaid with the sampling grid (80 by 120 mm, 10-by-10-mm grid size). The center of the sediment surface is covered by whitish veils built up by NivaVib1. (B) Distribution patterns of all sulfide gradient bacteria abundant at the time point of investigation (given in cell numbers per 0.1 ml).

flagella rotate in opposite directions, the cell body necessarily must form a right-handed helix in order that the propulsive forces of the cell body and the trailing flagellum act in the same direction (Fig. 5). Thus, a right-handed helix should be a common feature for spirilla, as we confirmed for the spirilla in the present study. The rotation of the leading flagellum, which is bent back along the cell body, provides additional torque to the cell body. Interestingly, the flagellar motors at the two ends of

the spirillum must always rotate in opposite directions (Fig. 5). This asymmetry necessarily requires some intracellular control mechanism, which may be unique for spirilla. A reversal in swimming direction consists of the sequence (i) stopping of all flagellar motors, (ii) resting for 20 to 140 ms, and finally (iii) starting of all flagellar motors in the opposite direction. The main propulsion force is apparently provided by the helical cell body; otherwise, the trailing flagellum would not be able to unfold after a reversal has taken place (Fig. 6).

At low Reynolds numbers the relation between cell rotation rate r and swimming speed v should theoretically show a linear dependence (32, 33), i.e., $v = kr$, where k is a constant. Our data agree with this very well (Fig. 4), showing that each spirilloid morphotype has its specific constant k. For comparison, the data obtained for the freshwater spirillum *Spirillum volutans* obtained by Ramia and Swan are also shown (34) (Fig. 4). *S. volutans* is morphologically similar to NivaSpi3. In the limit of very high viscosities of the surrounding medium, one full rotation of the cell body should result in a displacement equivalent to one period p of the spirilloid cell body. This implies that the constant k should be equal to p. However, due to the finite viscosity of water, measured values of k (Fig. 4) were generally smaller than the respective values for p (Table 1). This allows the definition of the slip $s = 1–kp^{-1}$, where $s = 0$ represents no slip and $s = 1$ corresponds to 100% slip (i.e., the cell is rotating but does not translate). According to this definition, the spirilla NivaSpi1, NivaSpi2, and NivaSpi3 show s slips of 0.45, 0.72, and 0.71, respectively. The cell shape of NivaSpi1 is characterized by a comparably large diameter of the helix in relation to the diameter of the cell body (Fig. 1). This might explain why this spirillum moves more efficiently, i.e., with less slip than the other spirilla. However, quantitative investigations of the efficiency (i.e., the fraction of the flagellar motor power which is converted into lateral movement) involve more complex considerations (32).

Temporal and spatial heterogeneity. The observed heterogeneous spatial distribution of microaerophilic bacteria in our enrichment cultures (Fig. 8) can be explained by locally differing oxygen gradients. The white veils formed by NivaVib1 in the center of the enrichment culture (Fig. 8A) indicate an oxic-anoxic interface positioned some millimeters above the sediment surface. Toward the borders of the enrichment culture, the position of the interface shifts downward, finally lying within the upper sediment layer, as can be anticipated by the bright sandy sediment surface. This is reflected by the distribution of the different species of colorless sulfur bacteria. The center of the enrichment culture is predominantly inhabited by NivaVib1, NivaSpi5, and NivaVib2. This region is surrounded by a region where "*Ca*. Ovobacter" is very abundant, which indicates that "*Ca*. Ovobacter" prefers regions where the oxic-anoxic interface lies very close to the sediment surface. Finally, *Beggiatoa* spp. and *Achromatium* sp., both relying on surface-associated motility, are found in regions where the oxic-anoxic interface is positioned within the sediment.

Another factor determining the spatial heterogeneity is the steepness of the oxygen gradient. As already discussed above, NivaVib1 can only aggregate at locations with oxygen gradients steeper than ca. 30 μM mm^{-1} (39), whereas the spirilla will also inhabit locations with oxygen gradients as low as 3 μM mm^{-1}.

Diversity of species and ecological significance. A diversity of free-swimming colorless sulfur bacteria has been described in the literature. Considering only neutrophilic and mesophilic species, they can be divided into aerotolerant and microaerophilic ones. The first group, comprising the genera *Thiobacillus*, *Thiomicrospira*, and *Thiosphaera*, is by far the best described because these organisms can be easily isolated and grown in pure cultures (28). The culture conditions do not require specially prepared chemical gradients; typically, homogeneously mixed thiosulfate and dissolved oxygen serve as the main substrates. The members of these species are average in size (several micrometers). Although they have been reported to exhibit flagellar motility, few studies of their motility and chemotactic behavior exist (8). However, because they have a size comparable to *Eschericia coli*, their swimming speeds are expected not to exceed 100 μm s^{-1}, and their chemotaxis is expected to involve "run and tumble."

The second group, comprising the microaerophilic species, has been termed "morphologically conspicuous sulfur-oxidizing bacteria" (29). Due to their relatively large size (>5 μm) and their frequently unusual morphology, members of this group have been described since the early days of microbiology, e.g., *Thiovulum* or *Thiospira* (10, 11, 17). The recently described species "*Ca*. Ovobacter" (20) and a large vibrioid bacterium (designated NivaVib1 here) (40) should be added to this group since they share a common ecological niche. Together with all of the other morphotypes described in the present study, all of these bacteria inhabit a thin layer in which oxygen and sulfide coexist on top of the sulfidic sediment. This may explain why all of these bacteria are relatively large: they are much less affected by Brownian motion than normal-sized bacteria (13), and they can achieve higher swimming speeds (up to 1,000 μm s^{-1}) (20). The diminished Brownian motion enables them to develop sophisticated motility strategies, whereas the high speeds let them cope with advective water currents on the sediment surface (30).

Altogether, the two described groups should be found in two different habitats. The aerotolerant species should predominate in habitats where advective mixing of oxygen and reduced sulfur compounds takes place: e.g., black smokers (36), chemocline in lakes (37), and leaching in mines rich in ferrous sulfide (22). The microaerophilic species should predominate in aquatic benthic habitats where solute transport is predominantly governed by diffusion and thus a thin microoxic zone develops (23). Only few examples of this group of organism have been isolated in pure culture thus far (see, for example, reference 11). We hope that our findings will encourage attempts to isolate additional members of this group. Supporting information and movies can be accessed online (http://www.mbl.ku.dk/mkuhl/DSGC).

ACKNOWLEDGMENTS

We thank Marianne Saietz for technical assistance and Anni Glud for manufacturing the microsensors.

This study were supported by grants to R.T. from the Danish Natural Science Research Council (project 57350) and the EU project PHOBIA and to T.F. from the Danish Natural Science Research Council and the Carlsberg Foundation.

REFERENCES

1. **Armitage, J. P., and H. L. Packer.** 1998. Bacterial motility and chemotaxis, p. 1–24. *In* D. R. Soll and D. W. Wessels (ed.), Motion analysis of living cells. Wiley, New York, N.Y.
2. **Barbara, G. M., and J. G. Mitchell.** 2003. Bacterial tracking of motile algae. FEMS Microbiol. Ecol. **44:**79–87.
3. **Barbara, G. M., and J. G. Mitchell.** 1996. Formation of 30- to 40-micrometer-thick laminations by high-speed marine bacteria in microbial mats. Appl. Environ. Microbiol. **62:**3985–3990.
4. **Barbara, G. M., and J. G. Mitchell.** 2003. Marine bacterial organisation around point-like sources of amino acids. FEMS Microbiol. Ecol. **43:**99–109.
5. **Berg, H. C.** 1993. Random walks in biology. Princeton University Press, Princeton, N.J.
6. **Berg, H. C.** 2003. The rotary motor of bacterial flagella. Annu. Rev. Biochem. **72:**19–54.
7. **Berg, H. C., and D. A. Brown.** 1972. Chemotaxis in *Escherichia coli* analysed by three-dimensional tracking. Nature **239:**500–504.
8. **Chakraborty, R., and P. Roy.** 1992. Chemotaxis of chemolithotrophic *Thiobacillus ferrooxidans* toward thiosulfate. FEMS Microbiol. Lett. **98:**9–12.
9. **Chwang, A. T., T. Y. Wu, and H. Winet.** 1972. Locomotion of spirilla. Biophys. J. **12:**1549–1550.
10. **De Boer, W. E., J. W. M. La Rivière, and A. L. Houwink.** 1961. Observations on the morphology of *Thiovulum majus* Hinze. Antonie Leeuwenhoek **27:** 447–456.
11. **Dubinina, G. A., and M. Y. Grabovich.** 1983. Isolation of pure *Thiospira* cultures and investigation of their sulfur metabolism. Microbiol. **52:**1–7.
12. **Dubinina, G. A., M. Y. Grabovich, A. M. Lysenko, N. A. Chernykh, and V. V. Churikova.** 1993. Revision of the taxonomic position of colorless sulfur spirilla of the genus *Thiospira* and description of a new species *Aquaspirillum bipunctata* nov. Microbiology **62:**638–644.
13. **Dusenbery, D. B.** 1997. Minimum size limit for useful locomotion by free-swimming microbes. Proc. Natl. Acad. Sci. USA **94:**10949–10954.
14. **Emerson, D., and C. Moyer.** 1997. Isolation and characterization of novel iron-oxidizing bacteria that grow at circumneutral pH. Appl. Environ. Microbiol. **63:**4784–4792.
15. **Emerson, D., and N. P. Revsbech.** 1994. Investigation of an iron-oxidizing microbial mat community located near Aarhus, Denmark: field studies. Appl. Environ. Microbiol. **60:**4022–4031.
16. **Emerson, D., and N. P. Revsbech.** 1994. Investigation of an iron-oxidizing microbial mat community located near Aarhus, Denmark: laboratory studies. Appl. Environ. Microbiol. **60:**4032–4038.
17. **Fauré-Fremief, E., and C. Roiller.** 1958. Étude microscope électronique d'une bactérie sulfureuse, *Thiovulum majus* Hinze. Exp. Cell Res. **14:**29–46.
18. **Fenchel, T.** 1969. The ecology of marine microbenthos IV. Structure and function of the benthic ecosystem, its chemical and physical factors and the microfauna communities with special reference to the ciliated protozoa. Ophelia **6:**1–182.
19. **Fenchel, T.** 1994. Motility and chemosensory behaviour of the sulphur bacterium *Thiovulum majus*. Microbiology **140:**3109–3116.
20. **Fenchel, T., and R. Thar.** 2004. "*cand*. Ovobacter propellens": a large conspicuous prokaryote with an unusual motility behaviour. FEMS Microbiol. Ecol. **48:**231–238.
21. **Head, I. M., N. D. Gray, H. Babenzien, and F. Oliver Glöckner.** 2000. Uncultured giant sulfur bacteria of the genus *Achromatium*. FEMS Microbiol. Ecol. **33:**171–180.
22. **Holmes, P. R., T. A. Fowler, and F. K. Crundwell.** 1999. The mechanism of bacterial action in the leaching of pyrite by *Thiobacillus ferrooxidans*. J. Electrochem. Soc. **146:**2906–2912.
23. **Jørgensen, B. B.** 1994. Diffusion processes and boundary layers in microbial mats, p. 243–253. *In* L. J. Stal and P. Caumette (ed.), Microbial mats, vol. 35. Springer, New York, N.Y.
24. **Jørgensen, B. B.** 1982. Ecology of the bacteria of the sulphur cycle with special reference to anoxic-oxic interface environments. Phil. Trans. R. Soc. Lond. B **298:**543–561.
25. **Jørgensen, B. B.** 1988. Ecology of the sulphur cycle: oxidative pathways in sediments, p. 31–63. *In* J. A. Coles and S. J. Ferguson (ed.), The nitrogen and sulfur cycles. Cambridge University Press, Cambridge, United Kingdom.
26. **Jørgensen, B. B.** 2001. Life in the diffusive boundary layer, p. 348–373. *In* B. P. Boudreau and B. B. Jørgensen (ed.), The benthic boundary layer. Oxford University Press, New York, N.Y.
27. **Jørgensen, B. B., and N. P. Revsbech.** 1983. Colorless sulfur bacteria, *Beggiatoa* spp. and *Thiovulum* spp., in O_2 and H_2S microgradients. Appl. Environ. Microbiol. **45:**1261–1270.
28. **Kuenen, J. G., L. A. Robertson, and O. H. Tuovinen.** 1992. The genera *Thiobacillus*, *Thiomicrospira*, and *Thiosphaera*, p. 2638–2657. *In* A. Balows, H. G. Trüper, M. Dworkin, W. Harder, and K.-H. Schleifer (ed.), The prokaryotes, vol. 3. Springer, New York, N.Y.
29. **La Rivière, J. W. M., and K. Schmidt.** 1992. Morphologically conspicuous sulfur-oxidizing eubacteria, p. 3934–3947. *In* A. Balows, H. G. Trüper, M. Dworkin, W. Harder, and K.-H. Schleifer (ed.), The prokaryotes, vol. 4. Springer, New York, N.Y.
30. **Luchsinger, R. H., B. Bergersen, and J. G. Mitchell.** 1999. Bacterial swimming strategies and turbulence. Biophys. J. **77:**2377–2386.
31. **Møller, M. M., L. P. Nielsen, and B. B. Jørgensen.** 1985. Oxygen responses and mat formation by *Beggiatoa* spp. Appl. Environ. Microbiol. **50:**373–382.
32. **Purcell, E. M.** 1997. The efficiency of propulsion by a rotating flagellum. Proc. Natl. Acad. Sci. USA **94:**11307–11311.
33. **Purcell, E. M.** 1976. Life at low Reynolds number. Am. J. Phys. **45:**3–11.
34. **Ramia, M., and M. A. Swan.** 1994. The swimming of unipolar cells of *Spirillum volutans*: theory and observations. J. Exp. Biol. **187:**75–100.
35. **Revsbech, N. P.** 1989. An oxygen microelectrode with guard cathode. Limnol. Oceanogr. **34:**474–478.
36. **Rona, P. A., G. Klinkhammer, T. A. Nelsen, J. H. Trefry, and H. Elderfield.** 1986. Black smokers, massive sulfides and vent biota at the Mid-Atlantic Ridge. Nature **321:**33–37.
37. **Sorokin, Y. I.** 1970. Interrelations between sulphur and carbon turnover in leromictic (sic!) lakes. Arch. Hydrobiol. **66:**391–446.
38. **Thar, R., and T. Fenchel.** 2001. True chemotaxis in oxygen gradients of the sulfur-oxidizing bacterium *Thiovulum majus*. Appl. Environ. Microbiol. **67:** 3299–3303.
39. **Thar, R., and M. Kühl.** 2003. Bacteria are not too small for spatial sensing of chemical gradients: an experimental evidence. Proc. Natl. Acad. Sci. USA **100:**5748–5753.
40. **Thar, R., and M. Kühl.** 2002. Conspicuous veils formed by vibrioid bacteria on sulfidic marine sediment. Appl. Environ. Microbiol. **68:**6310–6320.
41. **Turner, L., W. S. Ryu, and H. C. Berg.** 2000. Real-time imaging of fluorescent flagellar filaments. J. Bacteriol. **182:**2793–2801.
42. **Wirsen, C. O., and H. W. Jannasch.** 1978. Physiological and morphological observations on *Thiovulum* sp. J. Bacteriol. **136:**765–774.